JTTEE5 14:397-404
DOI: 10.1361/105996305X59413
1059-9630/$19.00 © ASM International

Superior Performance of High-Velocity Oxyfuel-Sprayed Nanostructured TiO_2 in Comparison to Air Plasma-Sprayed Conventional Al_2O_3-13TiO_2

R.S. Lima and B.R. Marple

(Submitted October 7, 2004; in revised form January 18, 2005)

Air plasma-sprayed conventional alumina-titania (Al_2O_3-13wt.%TiO_2) coatings have been used for many years in the thermal spray industry for antiwear applications, mainly in the paper, printing, and textile industries. This work proposes an alternative to the traditional air plasma spraying of conventional alumina-titania by high-velocity oxyfuel (HVOF) spraying of nanostructured titania (TiO_2). The microstructure, porosity, hardness (HV 300 g), crack propagation resistance, abrasion behavior (ASTM G65), and wear scar characteristics of these two types of coatings were analyzed and compared. The HVOF-sprayed nanostructured titania coating is nearly pore-free and exhibits higher wear resistance when compared with the air plasma-sprayed conventional alumina-titania coating. The nanozones in the nanostructured coating act as crack arresters, enhancing its toughness. By comparing the wear scar of both coatings (via SEM, stereoscope microscopy, and roughness measurements), it is observed that the wear scar of the HVOF-sprayed nanostructured titania is very smooth, indicating plastic deformation characteristics, whereas the wear scar of the air plasma-sprayed alumina-titania coating is very rough and fractured. This is considered to be an indication of a superior machinability of the nanostructured coating.

Keywords abrasion resistance, air plasma spray, conventional alumina-titania, high-velocity oxyfuel, nanostructured titania

1. Introduction

Air plasma-sprayed conventional alumina-titania (Al_2O_3-13wt.%TiO_2) coatings have been known for many years in the thermal spray community for their antiwear applications. They are among the most well-known ceramic coatings in the thermal spray industry and academia. Many articles and information about alumina-titania coatings can be found in books (Ref 1), proceedings of thermal spray conferences (Ref 2), and refereed journals (Ref 3).

The attention of the scientific community has been focused on nanostructured materials since the end of the 1990s. Depending on the processing conditions, they can exhibit superior mechanical performance when compared with conventional materials (Ref 4-7). The processing of nanostructured materials has also reached the thermal spray community. It has also been demonstrated that nanostructured thermal spray coatings exhibit superior mechanical performance when compared with their conventional counterparts (Ref 8, 9).

A very well-known ceramic material that has largely not been investigated in the thermal spray literature is titania (TiO_2). Titania is considered to be a material that has moderate wear resistance, mainly due to its lower mechanical resistance, fracture toughness, and hardness when compared with other ceramics like alumina (Al_2O_3) (Ref 10).

However, from the processing point of view, titania is a very interesting material. For a ceramic material, it has a relatively low melting point, 1855 °C (Ref 11). Due to its low melting point, titania can be "easily" sprayed via air plasma spray (APS), vacuum plasma spray, oxyacetylene flame spray, and, depending on the spray parameters, even high-velocity oxyfuel (HVOF) (Ref 12, 13). Therefore, it is possible to engineer unique and different microstructures with this material. In fact, it has been demonstrated that HVOF-sprayed conventional titania coatings exhibit highly uniform microstructures, very low porosity (<1%), and a very uniform distribution of hardness values (Ref 12, 13).

It has been observed that HVOF-sprayed nanostructured titania coatings exhibit higher wear resistance and higher bond strength when compared with conventional titania coatings sprayed via APS and HVOF (Ref 14). As a consequence of these interesting results, it was decided that, due to the unique character of the feedstock (i.e., nanostructured) and the particular processing method used to spray the ceramic material (i.e., HVOF), it would be useful to compare the wear behavior of this nanostructured coating with that of a traditional air plasma-sprayed conventional alumina-titania coating, which is widely used in antiwear applications. The studies aim to show that the new approach of HVOF spraying of nanostructured titania merits consideration for replacing the traditional approach of air plasma spraying with conventional alumina-titania for producing coatings used in antiwear applications.

R.S. Lima and **B.R. Marple,** National Research Council of Canada, 75 de Mortagne Boulevard, Boucherville, QC, J4B 6Y4 Canada. Contact e-mail: rogerio.lima@cnrc-nrc.gc.ca.

Table 1 Summary of the optimization process of the air plasma-sprayed Al_2O_3-13wt.%TiO_2 coating (No. 9) employed in this study

Coating	Powder	Morphology	V, m/s	T, °C	I, A	Ar, lpm	H_2, lpm	Vickers, 300*g*
1	Nanoclad TA 100-SD(a)	Nanostructured	213	2519	500	50	0.6	706
2	Nanoclad TA 100-SD(a)	Nanostructured	236	2562	700	50	1.0	686
3	Nanoclad TA 100-SD(a)	Nanostructured	237	2687	800	50	1.6	680
4	Amperit 748.054(b)	Agglomerated	215	2515	500	50	1.0	760
5	Amperit 748.054(b)	Agglomerated	240	2597	700	50	1.5	832
6	Amperit 748.054(b)	Agglomerated	241	2682	800	50	2.2	907
7	Metco 130(c)	Clad	190	2276	500	50	0.6	861
8	Metco 130(c)	Clad	224	2556	700	50	0.8	959
9	Metco 130(c)	Clad	223	2700	800	50	1.6	1080

(a) Nanophase, Burr Ridge, IL.
(b) H.C. Starck GmbH, Goslar, Germany.
(c) Sulzer Metco, Westbury, NY.

2. Experimental Method

2.1 Thermal Spraying and Particle Diagnostics

Nanostructured titania (TiO_2) feedstock (Altair VHP-DCS [5-20 μm]; Altair Nanomaterials Inc., Reno, NV) having a nominal particle size range of 5 to 20 μm was sprayed using an HVOF torch (Diamond Jet 2700-hybrid, Sulzer Metco, Westbury, NY). The conventional alumina-titania (Al_2O_3-13wt.%TiO_2) feedstock (Metco 130; Sulzer Metco, Westbury, NY) having a nominal particle size range from 15 to 53 μm was sprayed using an APS torch (SG100; Praxair, Indianapolis, IN). The particle temperature and velocity of the feedstock powders in both spray jets were measured using a diagnostic tool (DPV 2000; Tecnar Automation, Saint Bruno, QC, Canada). The in-flight particle data were acquired at the spray distance at which the substrates would be positioned when depositing a coating (APS system 6.4 cm; HVOF system 20 cm).

The coatings were deposited on low-carbon steel substrates that had been grit-blasted with alumina to roughen the surface before spraying. During the spraying process, a cooling system consisting of air jets was applied to reduce the coating temperature. The coating temperature was monitored during spraying using an optical pyrometer. The maximum temperatures during the process were ~270 and ~150 °C, respectively, for the HVOF-sprayed and air plasma-sprayed coatings. The typical coating thickness was 400 to 500 μm.

The HVOF-sprayed nanostructured titania coating had been previously optimized by developing spray conditions that produced high particle temperatures and velocities in the HVOF spray jet (Ref 14). The air plasma-sprayed alumina-titania coating that was chosen for comparison in this study was optimized by spraying three types (morphologies) of Al_2O_3-13wt.%TiO_2 particles (i.e., clad, agglomerated, and nanostructured). A total of nine different alumina-titania coatings were produced, and the one that exhibited the highest hardness was selected for subsequent comparison. The summary of the optimization process can be found in Table 1 (the sample selected for comparison in this study was coating No. 9).

2.2 Microstructural Characterization

The morphologies of the nanostructured titania feedstock and nonmolten nanostructured particles embedded in the coating microstructure were evaluated using a scanning electron microscope (SEM) at high magnification. The cross sections of the coatings were vacuum-impregnated with low-viscosity epoxy and were polished for study using the SEM. Coating porosity was evaluated on the cross section of the coatings using a SEM and image analysis. A total of 10 SEM pictures were analyzed for porosity measurements.

The wear scar of the coatings was analyzed via stereoscope microscopy and the SEM to observe the differences in scar smoothness. The roughness (Ra) of the wear scars was measured perpendicular to the abrasion direction to quantify the smoothness. A total of 10 Ra measurements were performed for each coating.

2.3 Mechanical Properties and Performance

Vickers hardness measurements were performed under a 300 *g* load for 15 s on the cross section of the coatings. A total of 10 indentations were performed on each coating. The crack propagation resistance was determined by indenting the coating cross section with a Vickers indenter at a load of 5 kg for 15 s, with the indenter aligned such that one of its diagonals would be parallel to the substrate surface. The total length of the major crack (*2c*) parallel to the substrate surface that originated at or near the corners of the Vickers indentation impression was measured. Based on the indentation load (*P*) and *2c*, the crack propagation resistance was calculated according to the relation between load and crack length $P/c^{3/2}$ (Ref 15), where *P* is in Newtons and *c* is in meters. All indentation cracks were significantly larger than the diagonal length of the indentation impression (*2a*) (i.e., $c \geq 2a$). Therefore, it is assumed that these cracks had half-penny geometry (Ref 15). All of the indentations were performed very near the centerline of the cross section, and the average of five indentations was taken for crack propagation resistance calculations.

The abrasion resistance of the coatings was tested based on the ASTM standard G65-00 (procedure D, modified) (Ref 16), which is also known as the dry sand/rubber wheel test. In this test, a stationary coated sample was pressed against a rotating rubber-coated wheel (diameter 228.6 mm; 200 rpm) with a force of 45 N. Silica sand (particle size 212–300 μm) was fed (300–400 g/min) between the coating and the rubber wheel until the wheel traveled over the equivalent linear distance of 1436 m. Prior to being tested, the surfaces of the coatings were prepared by grinding with diamond wheels to produce a leveled surface.

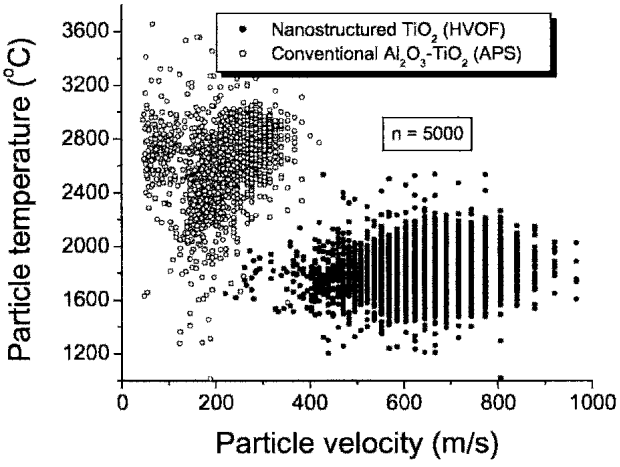

Fig. 1 Distribution of particle temperature and velocity in the spray jets for the nanostructured titania and conventional alumina-titania feedstock particles

Two samples were tested for each coating produced in this study. The volume of the material abraded away during the wear test was measured via optical profilometry.

3. Results and Discussion

3.1 In-Flight Particle Characteristics

Figure 1 shows the distribution of particle temperature and velocity in the spray jets for the nanostructured titania and conventional alumina-titania feedstock particles. The average particle temperature and velocity for the HVOF-sprayed nanostructured titania particles were 1814 ± 158 °C and 647 ± 101 m/s, respectively. The average particle temperature and velocity for the air plasma-sprayed conventional alumina-titania particles were 2700 ± 212 °C and 223 ± 46 m/s, respectively. Both spray parameters were optimized for the respective thermal spray systems and feedstock powders. For HVOF spraying, it was aimed to achieve particle temperatures close to the melting point of titania (i.e., 1855 °C) (Ref 11), which is a challenge due to the limitation imposed by the low temperatures of the HVOF flames, while still maintaining the typical high velocities of HVOF-sprayed particles. For plasma spraying, the objective was to produce, in addition to high temperatures, a high particle velocity (i.e., relatively for air plasma-sprayed particles). Both objectives, for HVOF and plasma spraying, were reached (Fig. 1).

Mainly due to the differences in particle temperature, the deposition efficiency (DE) of the air plasma-sprayed conventional alumina-titania coating is 58%, whereas the DE of the HVOF-sprayed nanostructured titania coating is 48%. The average particle temperature of the HVOF-sprayed nanostructured titania coating (1814 ± 158 °C) was close to the melting point of titania (1855 °C) (Ref 11). As previously mentioned, this was caused by the limitation of flame temperature for the HVOF torch and contributed to producing a lower DE. However, this temperature distribution close to the melting point of titania will contribute to keeping intact part of the original nanostructure of the feedstock embedded in the coating microstructure (i.e., not all particles will be fully molten). As already observed in earlier work (Ref 14), the presence of nonmolten nanostructured titania particles in the coating microstructure can enhance the mechanical performance of the coating.

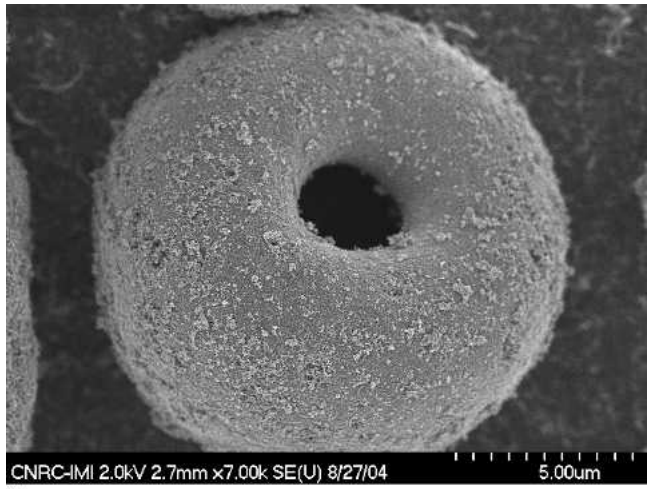

(a)

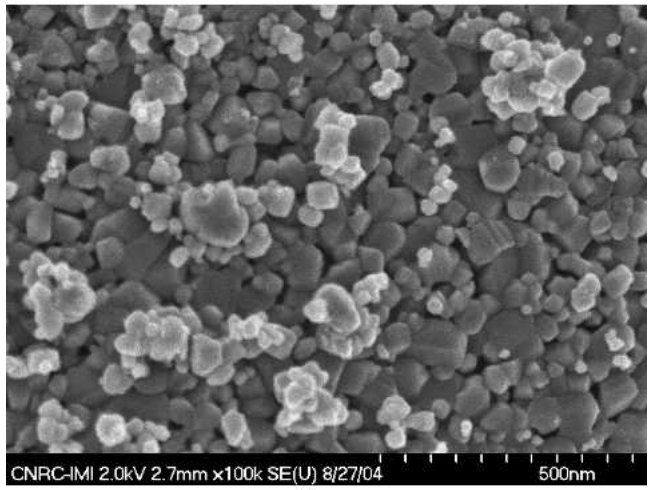

(b)

Fig. 2 (a) Microscopic titania particle formed by the agglomeration of individual nanosized particles of titania. (b) Particle from (a) observed in high magnification (individual nanosized titania particles are seen).

3.2 Nanostructure of the Feedstock

Figure 2(a) shows a typical particle of the nanostructured titania feedstock. It exhibits the typical donut shape of spray-dried particles. When analyzed at high magnification, it is possible to observe the nanostructure of the feedstock (Fig. 2b). Each microscopic feedstock particle is formed by the agglomeration via spray-drying of innumerable individual nanosized particles of titania. All individual nanosized particles of titania are smaller than ~100 nm.

3.3 Coating Porosity, Hardness and Crack Propagation Resistance

Table 2 shows the results of coating porosity, hardness, and crack propagation resistance. The HVOF-sprayed nanostruc-

Table 2 Porosity, Vickers hardness, and crack propagation resistance

Property	HVOF nanostructured TiO_2 coating	APS conventional Al_2O_3-13wt.%TiO_2 coating
Porosity, % (n = 10)	<1	1.9 ± 0.3
Vickers hardness, 300 *g* (n = 10)	810 ± 26	1080 ± 58
Crack propagation resistance, $MPam^{1/2}$ (n = 5)	26.8 ± 1.4	14.0 ± 2.5

tured titania coating is almost pore free. This characteristic is very important in applications where corrosion (in addition to wear) is an important issue. The air plasma-sprayed conventional alumina-titania coating is more porous, as would be expected for an air plasma-sprayed ceramic coating. Therefore, in applications where an abrasive and corrosive environment is found, a sealant may have to be used in this type of coating. It is important to point out that the application of a sealant does not necessarily guarantee corrosion protection. Sometimes the sealant slightly penetrates into the porosity of the coating, and during the grinding/polishing process it is pulled out from the coating microstructure leaving open channels toward the substrate surface. Sealant also may not be used in applications where high temperatures are present. Consequently, the nearly pore-free microstructure of the HVOF-sprayed nanostructured titania coating is an important advantage.

From Table 2, it is observed that the hardness of the air plasma-sprayed conventional alumina-titania coating is 33% higher than that of the HVOF-sprayed nanostructured titania. Despite the alumina-titania coating being more porous, the intrinsically higher degree of hardness of alumina (when compared with titania) makes it harder than the HVOF-sprayed nanostructured titania. Therefore, the presence of nanostructured zones in the HVOF-sprayed coating does not cause an increase in hardness; in fact, the hardness of the nanostructured coating is similar to that of HVOF-sprayed conventional titania (Ref 12, 13).

However, the results of crack propagation resistance show an opposite result. The crack propagation resistance of the nanostructured titania coating is almost twice that of the conventional alumina-titania coating. It is important to point out that the crack propagation resistance is a relative measure of the coating toughness; therefore, it may be stated that the HVOF-sprayed nanostructured titania coating is tougher than the air plasma-sprayed conventional alumina-titania coating. It will be seen in the next sections that the nanostructured zones in the HVOF-sprayed titania coating act as crack arresters, increasing coating toughness.

It is important to point out that the mean Vickers hardness (300*g*) of the alumina-titania coating was 1080 ± 58. The Vickers hardness values (300*g*) of plasma-sprayed alumina-titania coatings described by Westgard et al. (Ref 17), Luo et al. (Ref 18), and Pawloswski (Ref 1) are also ~1000. These studies represent five alumina-titania coatings produced by different laboratories around the world. Therefore, these results show that the hardness of the relatively high-density alumina-titania coating selected and tested in this study is equivalent to that of the typical coatings documented in the literature.

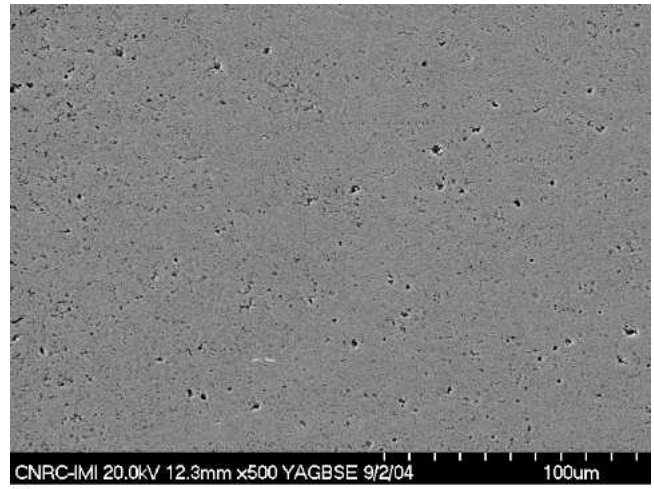

Fig. 3 (a) The cross section of the HVOF-sprayed nanostructured titania coating. (b) A nanostructured zone (originating from a semimolten particle) embedded in the microstructure of the HVOF-sprayed nanostructured titania coating

3.4 Coating Microstructure

Figure 3(a) shows the microstructure of the HVOF-sprayed nanostructured titania coating. The coating is very dense and uniform, not exhibiting the typical splat or layered structure of thermal spray coatings (i.e., the coating microstructure is similar to that of a bulk ceramic material). Thermal spray coatings are known for their anisotropic microstructure (Ref 19); however, in the case of the HVOF-sprayed nanostructured titania, it may be stated that this coating exhibits an isotropic microstructure.

When observing the HVOF-sprayed nanostructured titania coating via SEM in high magnification, it is possible to observe the nanostructured zones. The nanostructured zones correspond to particles that were semimolten in the spray jet and became embedded in the coating microstructure. Figure 3(b) shows a typical nanostructured zone. The nanostructured zone is very well embedded (i.e., no microstructural gaps) in the coating microstructure and is surrounded by particles that were fully mol-

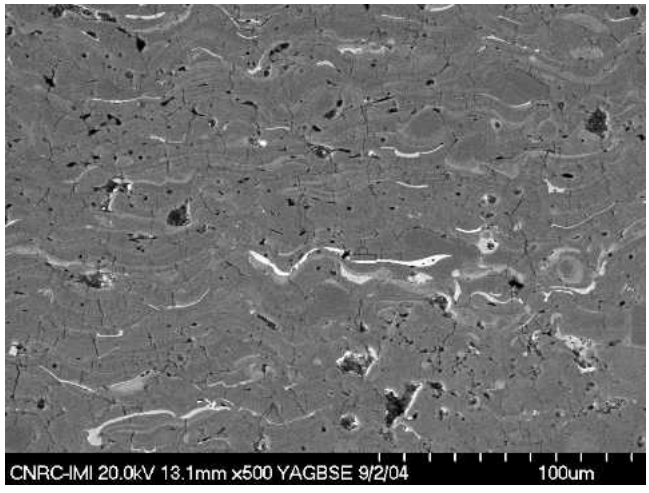

Fig. 4 The cross section of the air plasma-sprayed conventional alumina-titania coating

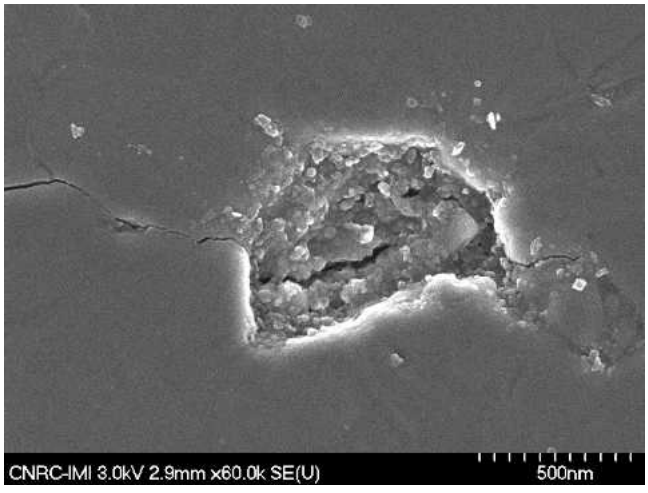

Fig. 5 An indentation crack arrested by a nanostructured zone in the HVOF-sprayed nanostructured titania coating

Table 3 Volume loss during abrasion test

Coating	Volume loss, mm^3 (n = 2)
HVOF nanostructured TiO_2	14.7 ± 0.2
APS conventional Al_2O_3-13wt.%TiO_2	20.0 ± 2.1

ten during spraying. The particles found in this zone are <100 nm, and it is possible to observe the similarity between the nanostructures of this zone and those of the feedstock particle (Fig. 2b). It is important to point out that nanostructured zones like that of Fig. 3(b) are found randomly dispersed throughout the coating microstructure.

Figure 4 shows the microstructure of the air plasma-sprayed conventional alumina-titania coating. The microstructure exhibits the typical layered structure of thermal spray coatings. The presence of pores and a network of microcracking are also observed. This cracking was probably caused by stress relaxation of the molten particles during solidification and cooling (Ref 20).

3.5 Abrasion Resistance

Table 3 shows the volume loss for the HVOF-sprayed nanostructured titania coating and for the air plasma-sprayed conventional alumina-titania coating in abrasion tests. The HVOF-sprayed nanostructured titania coating exhibits higher wear resistance, with 27% less volume loss than exhibited by the air plasma-sprayed alumina-titania coating under the same abrasive conditions. It is important to point out that titania coatings are usually considered to have moderate wear resistance, whereas alumina-titania coatings are usually considered to be of superior wear resistance.

It is important to recall that the hardness of the air plasma-sprayed conventional alumina-titania coating is 33% higher than that of the HVOF-sprayed nanostructured titania (Table 2). However, this higher hardness did not translate into better wear performance.

Another work of the present authors concluded that the nanostructured zones in the HVOF-sprayed nanostructured titania act as crack arresters by impeding crack propagation, which increases coating toughness (Ref 14). This phenomenon of toughness enhancement by the presence of nanozones was also observed by other authors with nanostructured thermal spray coatings (Ref 8). In conventional coatings, the well-defined splat boundaries provide easy crack propagation paths. In nanostructured coatings, the splat boundary structure is disrupted by the nanozones, which can help to arrest crack propagation. The increased crack propagation resistance (or relative toughness) of the HVOF-sprayed nanostructured titania (which also exhibits a relatively high hardness) is responsible for its higher wear resistance. Figure 5 shows an example of a crack arresting near a nanostructured zone in the HVOF-sprayed nanostructured titania coating. A Vickers indentation crack loses its energy and is arrested by passing through the nanostructured zone. Once again, it is important to point out that the nanostructured zones are randomly distributed and very well embedded in the dense and uniform coating microstructure; the cracks do not skirt them, and they act as crack arresters (i.e., energy absorbers). The increased toughness of the HVOF-sprayed nanostructured titania is then the main agent that is causing the enhanced wear resistance. The work of Liu et al. (Ref 21) shows the importance of toughness during the abrasion wear of ceramic thermal spray coatings.

3.6 Surface Morphology of the Wear Scar

Figures 6 and 7 show stereoscope microscope pictures of the surface of the wear scar for the HVOF-sprayed nanostructured titania coating and air plasma-sprayed conventional alumina-titania coating, respectively. It is possible to observe that the morphology of the wear scar of the HVOF-sprayed nanostructured titania coating is much smoother than the morphology of the wear scar of the air plasma-sprayed coating. This higher smoothness in the wear scar of nanostructured coatings when compared with that of conventional coatings has also been observed by other authors (Ref 8).

Figures 8 and 9 show SEM pictures taken at 45° to the surface

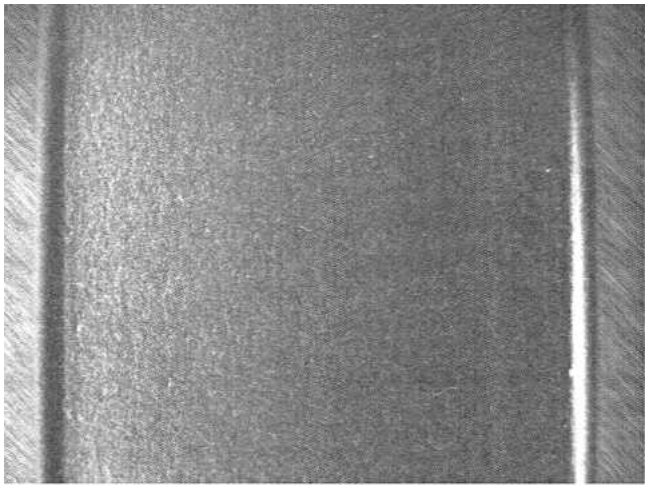

Fig. 6 Wear scar of the HVOF-sprayed nanostructured titania coating (the width of the wear scar is ~1.3 cm)

Fig. 7 Wear scar of the air plasma-sprayed conventional alumina-titania coating (the width of the wear scar is ~1.3 cm)

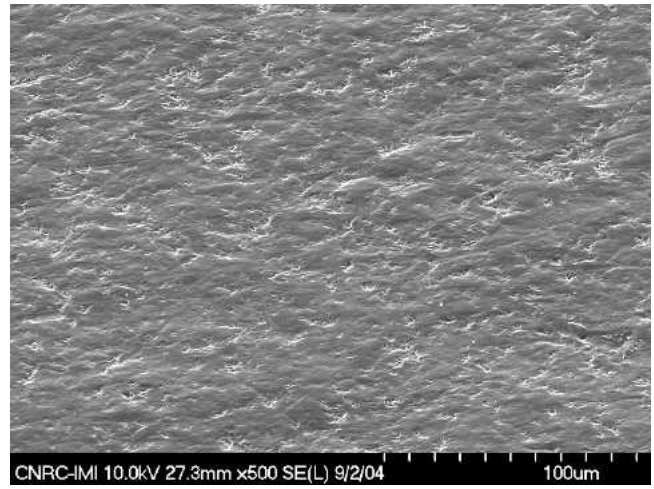

Fig. 8 SEM picture (taken at 45°) of the wear scar of the HVOF-sprayed nanostructured titania coating

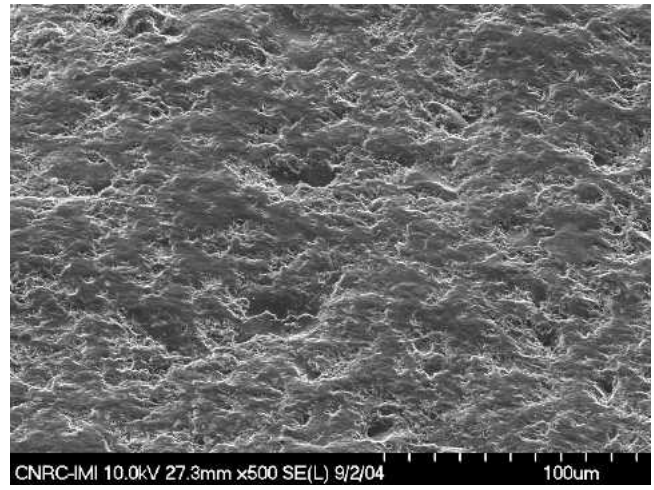

Fig. 9 SEM picture (taken at 45°) of the wear scar of the air plasma-sprayed conventional alumina-titania coating

of the wear scar of the two coatings. The wear scar morphology of the HVOF-sprayed nanostructured titania coating resembles a plastically deformed surface, whereas, the wear scar of the air plasma-sprayed conventional alumina-titania coating seems very fractured.

The Ra measurements (Table 4) also demonstrate the same characteristics observed in Fig. 6 to 9. The wear scar of the HVOF-sprayed nanostructured titania has a Ra that is 70% lower than that of the air plasma-sprayed conventional alumina-titania coating that was tested under the same abrasive conditions. Based on these above-described characteristics, it is assumed that the HVOF-sprayed nanostructured titania coating would exhibit superior machinability.

It has been shown that plastic deformation (i.e., ductile flow) and fragmentation (i.e., brittle fracture) occur during the grinding of thermal spray ceramic coatings (Ref 22). During the grinding of a ceramic material, a transition of the material removal mechanism from ductile mode to brittle mode occurs. The initial ductile flow progressively changes to brittle fracture after a critical depth of cut is reached. The critical depth of cut of a ceramic material is directly proportional to its toughness-to-hardness ratio (Ref 22). Therefore, the HVOF-sprayed nanostructured titania coating, which shows lower hardness (when compared with air plasma-sprayed conventional alumina-titania coating) and higher toughness, should exhibit a higher critical depth of cut. This higher critical depth of cut (i.e., a large region for plastic deformation) should translate into a smoother wear scar (as observed) and a higher machinability. This enhanced plasticity of the HVOF-sprayed nanostructured titania coating

Table 4 Roughness of the wear scar

Coating	Ra (n = 10)
HVOF nanostructured TiO_2	0.06 ± 0.02 μm
APS conventional Al_2O_3-13wt.%TiO_2	0.21 ± 0.11 μm

(and its relatively high hardness) should allow more energy absorption during wear, contributing to a lowering of the volume loss during abrasion (Table 3) (i.e., an increase in wear resistance).

During the processing of ceramic thermal spray coatings for antiwear applications, machining of the coating (i.e., grinding and polishing) is normally required. This process can be very expensive and time consuming. Therefore, the use of an HVOF-sprayed nanostructured titania coating constitutes a very important advantage.

3.7 Final Comments

One may argue that a comparison between the air plasma-sprayed alumina-titania coating with an HVOF-sprayed alumina-titania coating would be of more scientific fairness. However, due to the higher melting point of Al_2O_3-13wt.%TiO_2 (~2000 °C) (Ref 23) when compared with that of TiO_2 (1855 °C) (Ref 11), it is very difficult to use HVOF to spray the alumina-titania coating using the HVOF torch DJ2700-hybrid (the one used in this work) and have acceptable DE values. In fact, during the course of this work, the HVOF spraying of alumina-titania was attempted, and the results for DE were unimpressive.

It is important to recall that earlier work demonstrated that the HVOF-sprayed nanostructured titania coating exhibits higher wear resistance when compared with air plasma-sprayed and HVOF-sprayed conventional titania coatings (Ref 14). Consequently, the choice and use of the HVOF-sprayed nanostructured titania coating seems to be appropriate for further comparisons of wear behavior with other ceramic coatings.

Therefore, from an engineering point of view, the comparison of an air plasma-sprayed conventional alumina-titania coating (traditional method) with an HVOF-sprayed nanostructured titania coating (new method) is of practical validity. And it is also important to point out that the HVOF torch DJ2700-hybrid is very popular in North American laboratories and thermal spray job shops. Consequently, this research can offer an interesting alternative, a new option, and new perspectives on antiwear applications for various students, researchers, and engineers who are DJ2700-hybrid users.

4. Conclusions

- Although titania is considered to be a coating of moderate wear resistance, when it is made from a nanostructured feedstock and is HVOF-sprayed, it exhibits a superior abrasion wear resistance (27% lower volume loss) when compared with an air plasma-sprayed conventional alumina-titania coating (which is normally considered to be a coating with high wear resistance).
- The air plasma-sprayed conventional alumina-titania coating is 33% harder than the HVOF-sprayed nanostructured titania; however, this higher hardness does not translate into better performance.
- The HVOF-sprayed nanostructured titania coating exhibits a crack propagation resistance that is almost twice that of the air plasma-sprayed conventional alumina-titania coating (i.e., the nanostructured coating is tougher than the conventional one).
- The HVOF-sprayed nanostructured titania coating exhibits a very dense (nearly pore free) and uniform isotropic microstructure (not exhibiting the typical layered structure of thermal spray coatings). This nearly pore-free microstructure is thought to be very useful in applications where corrosion (in addition to wear) is present.
- The higher wear resistance of the HVOF-sprayed nanostructured titania is provided by the nanostructured zones embedded in the dense and uniform coating microstructure. These nanozones do not increase the coating hardness; instead, they act as crack arresters, thereby increasing the toughness of the coating.
- The Ra of the wear scar of the HVOF-sprayed nanostructured titania is 70% lower than that of the air plasma-sprayed conventional alumina-titania coating when tested under the same abrasive conditions. This is considered to be an indication of higher machinability of the nanostructured coating, which is a desirable characteristic during the step of grinding and polishing of thermal spray coatings.
- The smoother wear scar of the nanostructured coating is probably the result of its higher critical depth of cut, which provides a broader plastic deformation range than that exhibited by the conventional coating. This enhanced ductility (while still maintaining a relatively high hardness) allows more energy absorption during wear, contributing to a lowering of the volume loss during abrasion (i.e., an increase in wear resistance).
- The abrasion wear test and microstructural characteristics evaluated in this work indicate that the HVOF-sprayed nanostructured titania coating exhibits a superior performance when compared with an air plasma-sprayed conventional alumina-titania coating. The results indicate that the new approach (i.e., HVOF-spraying of nanostructured titania) merits consideration for replacing the traditional approach (i.e., air plasma spraying of conventional alumina-titania) for antiwear applications.

Acknowledgments

Part of the results of this article originated from research funded by Altair Nanomaterials Inc. The authors thank Altair Nanomaterials Inc. for encouraging the publication of these results. The authors also thank S. Belanger and F. Belval for APS and HVOF spraying, M. Lamontagne for the DPV2000 measurements, J.F. Alarie for metallography, and M. Thibodeau for the SEM pictures.

References

1. L. Pawlowski, *The Science and Engineering of Thermal Spray Coatings,* Wiley, West Sussex, UK, 1995
2. T. Varis, E. Rajamaki, and K. Korpiola, Mechanical Properties of Thermal Spray Coatings, *Thermal Spray 2001: New Surfaces for a New Millenium,* C.C. Berndt, K.A. Khor, and E.F. Lugscheider, Ed., May 28-30, 2001 (Singapore), ASM International, 2001, p 993-997
3. M. Bounazef, S. Guessasma, G. Montavon, and C. Coddet, Effect of APS Process Parameters on Wear Behavior of Alumina-Titania Coatings, *Mater. Lett.,* Vol 58, 2004, p 2451-2455
4. C. Suryanarayana, The Structure and Properties of Nanocrystalline Materials: Issues and Concerns, *J. Metals,* (September), 2002, p 24-27
5. M.J. Mayo, R.W. Siegel, A. Narayanasamy, and W.D. Nix, Mechanical

Properties of Nanophase TiO_2 as Determined by Nanoindentation, *J. Mater. Res.,* Vol 5 (No. 5), 1990, p 1073-1082
6. Y. Lu and P.K. Liaw, The Mechanical Properties of Nanostructured Materials, *J. Metals* (March), 2001, p 31-35
7. P.M. Ajayan and F. Banhart, Nanotubes: Strong Bundles, *Nat. Mater.,* Vol 3, 2004, p 135-136
8. M. Gell, E.H. Jordan, Y.H. Sohn, D. Goberman, L. Shaw, and T.D. Xiao, Development and Implementation of Plasma Sprayed Nanostructured Ceramic Coatings, *Surf. Coat. Technol.,* Vol 146-147, 2001, p 48-54
9. G.E. Kim, J. Walker, Jr., and J.B. Williams, Jr., Nanostructured Titania Coated Titanium, US Patent 6, 835, 449B2, December 28, 2004
10. R.L. Lehman, Overview of Ceramic Design and Process Engineering, *Engineered Materials Handbook*, Vol 4, *Ceramic and Glasses,* S.J. Schneider, Ed., ASM International, 1991, p 29-37
11. M. Miyayama, K. Koumoto, and H. Yanagida, Engineering Properties of Single Oxides, *Engineered Materials Handbook*, Vol. 4, *Ceramic and Glasses,* S.J. Schneider, Ed., ASM International, 1991, p 748-757
12. R.S. Lima and B.R. Marple, High Weibull Modulus HVOF Titania Coatings, *J. Thermal Spray Technol.,* Vol 12 (No. 2), 2003, p 240-249
13. R.S. Lima and B.R. Marple, Optimized HVOF Titania Coatings, *J. Thermal Spray Technol.,* Vol 12 (No. 3), 2003, p 360-369
14. R.S. Lima and B.R. Marple, From APS to HVOF Spraying of Conventional and Nanostructured Titania Feedstock Powders: A Study on the Enhancement of the Mechanical Properties, *Surf. Coat. Technol.,* 2005, in press
15. G.R. Anstis, P. Chantikul, B.R. Lawn, and D.B. Marshall, A Critical Evaluation of Indentation Techniques for Measuring Fracture Toughness: I. Direct Crack Measurements, *J. Am. Ceram. Soc.,* Vol 64 (No. 9), 1981, p 533-538
16. "Standard Test Method for Measuring Abrasion Using the Dry Sand/Rubber Wheel Apparatus," G65-00, *Annual Book of ASTM Standards,* ASTM 2000, p 1-12
17. R. Westergard, N. Axen, U. Wiklund, and S. Hogmark, An Evaluation of Plasma Sprayed Ceramic Coatings by Erosion, Abrasion and Bend Testing, *Wear,* Vol 246, 2000, p 12-19
18. H. Luo, D. Gobermann, L. Shaw, and M. Gell, Indentation Fracture Behavior of Plasma-Sprayed Nanostructured Al_2O_3-13wt.% TiO_2 Coatings. *Mater. Sci. Eng., A*, Vol 346, 2003, p 237-245
19. S.H. Leigh, C.K. Lin, and C.C. Berndt, Elastic Response of Thermal Spray Deposits under Indentation Tests, *J. Am. Ceram. Soc.,* Vol 80 (No. 8), 1997, p 2093-2099
20. S. Kuroda and T.W. Clyne, The Quenching Stress in Thermally Sprayed Coatings, *Thin Solid Films,* Vol 200, 1991, p 49-66
21. Y. Liu, T.E. Fischer, and A. Dent, Comparison of HVOF and Plasma-Sprayed Alumina/Titania Coatings: Microstructure, Mechanical Properties and Abrasion Behavior, *Surf. Coat. Technol.,* Vol 167, 2003, p 68-76
22. X. Liu, B. Zhang, and Z. Deng, Grinding of Nanostructured Ceramic Coatings: Surface Observations and Material Removal Mechanisms, *Int. J. Machine Tools Manufact.,* Vol 42, 2002, p 1665-1676
23. S.M. Lang, C.L. Fillmore, and L.H. Maxwell, System Al_2O_3-TiO_2, *Phase Diagram for Ceramists,* 3rd ed., E.M. Levin, C.R. Robins, and H.F. McMurdie, Ed., The American Ceramic Society, Columbus, OH, 1974